

Titolo

WPFC/AFCS Expert Group Benchmark on Dose Rate Calculations

Descrittori

Tipologia di documento: Technical Report
Collocazione contrattuale:
Argomenti trattati: Gamma dose rate

Sommario

This report describes ENEA's contribution to the WPCF/AFCS Expert Group benchmark on dose rate calculations. The results refer to the two parts in which the Benchmark is divided:

1. verification of the self-protection properties for spent PWR UOX and MOX fuel assemblies and code-to-code comparison of nuclide inventories and gamma dose rates;
2. validation of the gamma dose rates calculation strategy with the gamma dose rate measurements performed on a W15x15 UOX fuel assembly in 1981.

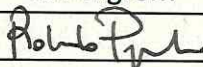

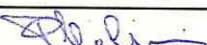
In the verification part, five different calculation strategies were simultaneously used to compare the performance of the codes. Overall, a good agreement between the five strategies in terms of nuclide inventories, gamma sources and gamma dose rates is observed.


In the validation part, the calculations were performed with Origen-S in the depletion and decay phases and MCNPX in the photon transport phase. The gamma dose rate values for the ANSI/ANS-6.1.1-1977 conversion factor are around 20% higher than those for the ANSI/ANS-6.1.1-1991 conversion factor. Compared to the measured values, the calculated ones differ at most -44% with the ANSI/ANS-6.1.1-1977 factor and -55% with the ANSI/ANS-6.1.1-1991 factor.

Autori: R. Pergreffi, F. Rocchi, A. Guglielmelli

Copia n.


In carico a:

2			NOME			
			FIRMA			
1	REVISIONE	15/07/2020	NOME	R. Pergreffi	F. Padoani	P. Meloni
			FIRMA			
0	EMISSIONE	16/01/2019	NOME	R. Pergreffi	F. Padoani	P. Meloni
			FIRMA			
REV.	DESCRIZIONE	DATA		REDAZIONE	CONVALIDA	APPROVAZIONE

 Centro Ricerche Bologna	Sigla di identificazione	Rev.	Distrib.	Pag.	di
	SICNUC-P000-026	1	L	2	34

Contents

1. Introduction.....	3
2. Verification part	4
2.1 Computational model	4
2.2 Codes and nuclear data libraries.....	7
2.2.1 Burnup and depletion phase.....	7
2.2.2 Decay and photon emission phase	9
2.2.3 Photon transport phase	9
2.3 Results	9
2.3.1 Results for UOX PWR fuel assembly.....	10
2.3.2 Results for MOX PWR fuel assembly.....	17
2.4 Sensitivity analysis.....	21
3. Validation part.....	23
3.1 Computational model	23
3.2 Codes and nuclear data libraries.....	24
3.2.1 Burnup and depletion phase.....	24
3.2.2 Decay and photon emission phase	24
3.2.3 Photon transport phase	24
3.3 Results	25
4. Conclusions.....	30
Appendix I – AINSI/ANS-6.1.1 Flux-to-dose conversion factors	31
Appendix II - Energy group structures.....	32
References.....	34
Acknowledgments.....	34

 Centro Ricerche Bologna	Sigla di identificazione	Rev.	Distrib.	Pag.	di
	SICNUC-P000-026	1	L	3	34

1. Introduction

Nowadays it is increasingly important to assess fuel assemblies (FAs) in terms of selfprotection properties against the risk of diversion and theft of nuclear material for illegal use.


The U.S. Nuclear Regulatory Commission (NRC) and International Atomic Energy Agency (IAEA) consider the self protecting dose rate to be 1 Sievert per hour (Sv/h) at 1 meter from a spent fuel assembly [US-DoE, 1997]. This is also the reference value used by the National Academy of Science (NAS) to consider the plutonium within a FA unattractive to theft [NAS, 1994].

Values of gamma dose rate in air at various distances and directions from light water reactor (LWR) fuel assemblies were calculated at the beginning of the 1990s [Lloyd, 1994]. For PWR UOX FAs irradiated up to 30,000 MWd/MTU, the value at 1 m perpendicular to the FA at the center varies between 198.15 and 7.88 Sv/h going from 1 to 50 years of decay.

Recently, some assessments performed by DOE and CEA [Feng, 2014] have suggested the need to check these values of gamma dose rate. In fact, they could be overestimated due perhaps to a very conservative calculation methodology typical of the radiation protection field. If so, this could represent a weakening of the intrinsic barrier against the risk of diversion. In order to determine the effective selfprotection of irradiated fuel assemblies, the **Advanced Fuel Cycle Scenarios** (AFCS) Expert Group, established in 2005 within the OECD's Nuclear Energy Agency, proposed a Benchmark in 2015 [Eschbach et al, 2015]. This benchmark is divided into two parts:

- a verification part, in which analytical calculations of nuclide inventories, gamma emissions and gamma dose rates for two irradiated PWR fuel assemblies after a 30 years period of decay, at 1 meter away from the axial midpoint, are performed;
- a validation part, in which the dose rate calculation strategy used in the previous part is validated with real cases.

The main results obtained by ENEA in both parts are discussed in this report.

 Centro Ricerche Bologna	Sigla di identificazione	Rev.	Distrib.	Pag.	di
	SICNUC-P000-026	1	L	4	34

2. Verification part

2.1 Computational model

The verification part of this benchmark deals with the calculation of:

- heavy metal (HM) masses [g] at discharge (EoL) and after a period of decay of 30 years;
- fission product (FP) masses [g] at discharge (EoL) and after a period of decay of 30 years;
- gamma photon release rates (and contributions from each energy group) at 1 m away from the axial midpoint after a period of decay of 30 years according to the schematic shown in Figure 1 where the gamma photon flux is tallied (the energy group structure is at user discretion);
- gamma dose rate after a period of decay of 30 years by using two flux-to-dose-rate conversion factors: ANSI/ANS-6.1.1-1977 and ANSI/ANS-6.1.1-1991.

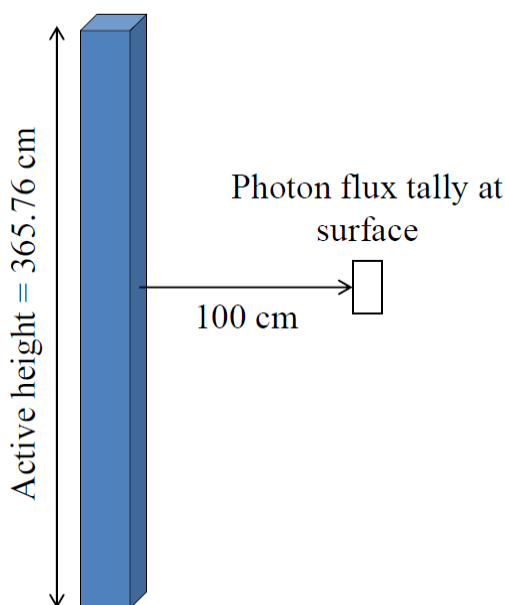
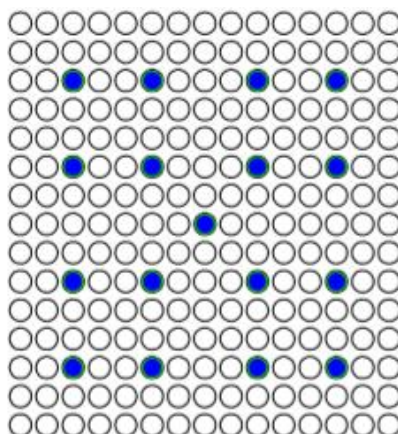


Figure 1. Schematic of gamma photon flux calculation.

For this part of the benchmark, two spent fuel assemblies are proposed: a 15x15 PWR UOX FA irradiated up to 33 MWd/kgHM and a 17x17 PWR MOX FA irradiated up to 60 MWd/kgHM. The main data of both fuel assemblies are reported below.

15x15 UOX PWR fuel assembly

The 15x15 UOX PWR FA, shown in Figure 2, is composed of 17 guide tubes and 208 fuel pins with a uniform initial enrichment of 3.11 wt% ²³⁵U. The guide tubes have been filled with water during irradiation. Material and geometrical data are given in Table 1.



- fuel pins (208)
- water tubes (17)

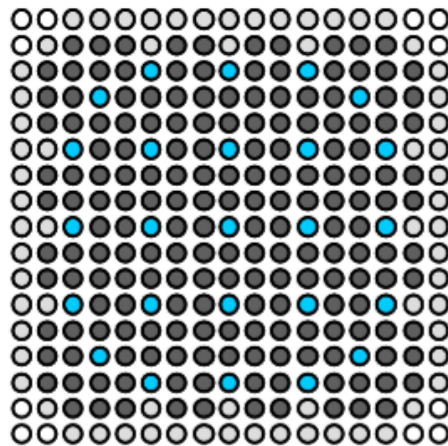
Figure 2. 15x15 UOX PWR FA.

Parameter	Value
Fuel pellet diameter [cm]	0.925
Cladding inner diameter [cm]	0.9398
Cladding outer diameter [cm]	1.0668
Guide tube inner diameter [cm]	1.242
Guide tube outer diameter [cm]	1.382
Pin pitch [cm]	1.4224
Active height [cm]	365.76
Assembly pitch [cm]	21.4
UO ₂ fuel density [g/cm ³]	10.412
Heavy metal mass [kgHM]	469.22
Fuel temperature [°C]	821
Clad temperature [°C]	342
Moderator temperature [°C]	305.6
Boron concentration [ppm]	456
²³⁵ U enrichment [wt%]	3.11
²³⁴ U concentration [ppm]	303
Specific power [W/g]	48
Burnup [MWd/kgHM]	33

Table 1. Assumed model parameters for 15x15 UOX PWR FA.

17x17 MOX PWR fuel assembly

The 17x17 MOX PWR FA, shown in Figure 3, is composed of 25 guide tubes and 264 fuel pins with three different Pu contents. The 25 guide tubes have been filled with water during irradiation. Material and geometrical data are given in Table 2. The plutonium vector in fresh MOX fuel is reported in Table 3.



- Low-Pu content pins
- Intermediate-Pu content pins
- High-Pu content pins
- Water tubes

Figure 3. 17x17 MOX PWR FA.

Parameter	Value
Fuel pellet diameter [cm]	0.8290
Cladding inner diameter [cm]	0.836
Cladding outer diameter [cm]	0.950
Guide tube inner diameter [cm]	1.142
Guide tube outer diameter [cm]	1.226
Pin pitch [cm]	1.26
Active height [cm]	365.76
Assembly pitch [cm]	21.58
UO ₂ fuel density [g/cm ³]	11.3
Heavy metal mass [kgHM]	454
Fuel temperature [°C]	620
Clad temperature [°C]	342
Moderator temperature [°C]	309
Boron concetration [ppm]	600
Low-Enr. Pu/HM [wt%]	3.65
Intermediate-Enr. Pu/HM [wt%]	6.49
High-Enr. Pu/HM [wt%]	9.77
Specific power [W/g]	41
Burnup [MWd/kgHM]	60

Table 2. Assumed model parameters for 17x17 MOX PWR FA.

Isotope	Weight percent [%]
²³⁸ Pu	2.62
²³⁹ Pu	52.67
²⁴⁰ Pu	25.45
²⁴¹ Pu	10.65
²⁴² Pu	7.54
²⁴¹ Am	1.07

Table 3. Plutonium vector in fresh MOX fuel.

2.2 Codes and nuclear data libraries

The gamma dose rate calculation is divided into three phases:

1. burnup and depletion;
2. calculation of decay and photon emission;
3. photon transport and evaluation of gamma dose rate.

In the verification part, five calculation strategies are simultaneously used in order to compare the performance of the codes. As detailed in Table 4, five different neutronic codes are used in the first phase, while the second and third phases are performed using Origen-S/Origen-ARP and MCNPX respectively.

Phase	Strategy 1	Strategy 2	Strategy 3	Strategy 4	Strategy 5
Burnup & depletion	APOLLO2	NEWT	SERPENT2	KENO-VI	Origen-ARP
Decay & Photon source	Origen-S	Orgigen-S	Origen-S	Origen-S	
Photon transport	MCNPX	MCNPX	MCNPX	MCNPX	MCNPX


Table 4. Computational tools.

A brief description of modeling tools and approaches used in each phase is provided below.

2.2.1 Burnup and depletion phase

APOLLO2.8-3.E

Microscopic cross sections refer to 281 groups master library with a SHEM group structure CEA2005V4.1.2.patch, based on JEFF 3.1.1 evaluations. Calculations are done assuming reflective boundary conditions and taking advantage of all symmetries of the system, so that only 1/8 of assembly is considered. Elementary fuel cell is divided into four concentric zones corresponding, from centre to periphery, to 50%, 30%, 15% and 5% of the total volume respectively, one clad zone and one moderator zone. Coherently with geometry, Collision Probability method (Pij method) is used to resolve the transport equation to compute the neutron flux. Selfshielding calculations are done taking into account the following isotopes: ²³⁸U, ²³⁵U, ²³⁹Pu, ²⁴⁰Pu, Zr_nat in both cases and Pu²⁴¹ only in the MOX case. Standard

 Centro Ricerche Bologna	Sigla di identificazione	Rev.	Distrib.	Pag.	di
	SICNUC-P000-026	1	L	8	34

depletion chain is extended to include higher minor actinides: Bk249, Cf249, Cf250, Cf251, and Cf252 using a CEA procedure, while Np236, Pu237, Pu243, and Am241 using an *ad hoc* procedure developed by ENEA. TR (all resonances) approximation is used over the entire energy range. The effect of leakage on the neutron spectrum is taken into account by means of homogenous B1 model that computes the buckling to assure criticality. Every 3 burn-up steps, self-shielding correction is recalculated and the working cross sections updated.

NEWT


Microscopic cross sections refer to V7-238 SCALE standard multigroup composition library based on the ENDF/B-VII.0 evaluation. Calculations are done dividing fuel area into five concentric zones of equal volume. The cross-sections processing is done by means of the CENTRM module: Bonami method for non-resolved range and CENTRM-PMC sequence for the resolved one. The multi-region cylindrical model for selfshielding calculations is selected. 230 nuclides (addnux=4) are added to the default t-depl set for performing a complete transmutation-decay chain evaluation of all benchmark nuclides. The flux calculation solver used is based on the discrete ordinate method. Convergence criteria are set to 1E-5 for criticality coefficient and 1E-4 for flux. CMFD is set equal to 4. b1 option for critical spectrum is used. For each depletion step, the self-shielding is recalculated and the cross section libraries updated.

SERPENT2.1.24

Microscopic cross sections refer to continuous energy cross sections libraries (ACE format) based on ENDF/B-VII.0 evaluated data files. Decay and nuclear fission yield data libraries are also based on ENDF/B-VII.0. The UO₂ fuel pin is modeled as a single volume zone. Thermal scattering data libraries for water is used. 62 nuclides are added in trace quantities in the initial material composition for performing a complete transmutation-decay chain evaluation of all benchmark nuclides. For the transport calculation, 300 cycles, with the first 50 inactive, each of which with 150000 particles is considered. Bateman equations are solved using the advanced matrix exponential solution [Chebyshev Rational Approximation Method (CRAM)]. The predictor-corrector method is used for the depletion calculation.

KENO-VI (t6-depl)

Microscopic cross sections refer to V7-238 SCALE standard multigroups composition library based on the ENDF/B-VII.0 evaluation. The UO₂ fuel pin is modeled in a single volume zone. The cross-sections processing is done by means of the CENTRM module. 230 nuclides (addnux=4) are added to the default t6-depl set for performing a complete transmutation-decay chain evaluation of all benchmark nuclides. The transport calculation is done by the multi-group Monte Carlo code (KENO VI) taking into account, for each burnup step, 300 cycles, with the first 50 inactive, each of which with 150000 particles. The burnup calculation is

 Centro Ricerche Bologna	Sigla di identificazione	Rev.	Distrib.	Pag.	di
	SICNUC-P000-026	1	L	9	34

automatically done by Origen-S. For each depletion step, the self-shielding is recalculated and the cross section libraries updated.

ORIGEN-ARP

The effective cross sections refer to the 1-grp W15x15 library prepared by ORNL using NEWT with 44-gr, LWR-optimized, micro-library based on ENDF/B-V evaluations. Density and temperature of water are set respectively to 0.7135 g/cm³ and 579 K. The boron concentration is equal to 653 ppm. The depletion chain includes 1946 linked nuclides. No cut-offs are used.

2.2.2 Decay and photon emission phase

ORIGEN-ARP

All photon emission calculations are performed using the 18-energy group structure contained in Appendix II. The bremsstrahlung due to decay only is included. 10 decay steps are taken into account.

2.2.3 Photon transport phase

MCNPX 2.7.0

The photon transport and dose rate calculations are performed using the photon library mcplib04. In this regard, it should be noted that, in both cases, the use of the mcplib84, the updating of mcplib04 photon Compton broadening data for MCNPX [White, 2012], does not produce any difference on gamma dose rate values. According to the benchmark specifications, no rim effect in the fuel pellet is taken into account. The photon source is uniformly distributed within the fuel pellet. The variance reduction is of type source bias for ERG distribution (imp=2 for energies above 0.4 MeV). Tallies type 4 over a 20x20x0.5 cm³ box at 1 m from FA center are used. Dose multiplier is of type DF for flux-to-dose rate conversion. For the 1991 ANSI/ANS standard, the anterior-posterior (AP) conversion factors are used. Secondary photons from (n,g) reactions are neglected. Bremsstrahlung due to secondary electrons is included with the Thick-Target Model. 1E+08 primary photons, corresponding to one standard deviation on the dose of about 3%, are used.

2.3 Results

The main results of this part are presented below distinguishing between the two fuel assemblies. In particular, Tables 5 to 11 refer to the UOX PWR FA while Tables 13 to 18 refer to MOX PWR FA. Table 12, at the end of the UOX case, shows the values of the gamma dose rates at 1 m from the midplane for a UOX FA after a period of decay of 3.7 y. The last section is dedicated to the assessment of the impact of some calculation options on the gamma dose rate.

2.3.1 Results for UOX PWR fuel assembly

Calculated Heavy Metal masses at EoL are shown in Table 5.

	APOLLO2	NEWT	Serpent	KENO-VI	Origen-Arp
U-234	8.14E+01	8.38E+01	8.31E+01	8.26E+01	8.19E+01
U-235	3.69E+03	3.83E+03	3.64E+03	3.93E+03	3.66E+03
U-236	1.80E+03	1.81E+03	1.81E+03	1.80E+03	1.83E+03
U-237	5.49E+00	5.77E+00	5.81E+00	5.90E+00	6.04E+00
U-238	4.43E+05	4.42E+05	4.43E+05	4.42E+05	4.43E+05
Np-236	5.24E-04	1.62E-04	6.88E-04	1.76E-04	7.91E-05
Np-236m	-	1.06E-05	2.86E-09	1.11E-05	4.05E-06
Np-237	1.75E+02	1.85E+02	1.84E+02	1.90E+02	1.88E+02
Np-238	7.83E-01	7.80E-01	7.78E-01	8.00E-01	8.42E-01
Np-239	5.92E+01	6.01E+01	5.94E+01	6.11E+01	5.90E+01
Pu-236	4.50E-04	6.96E-04	1.12E-05	7.31E-04	2.67E-04
Pu-237	1.29E-04	1.79E-04	1.56E-04	1.93E-04	1.55E-04
Pu-238	5.80E+01	5.73E+01	5.49E+01	5.97E+01	6.00E+01
Pu-239	2.51E+03	2.65E+03	2.45E+03	2.80E+03	2.52E+03
Pu-240	1.10E+03	1.11E+03	1.11E+03	1.13E+03	1.10E+03
Pu-241	6.32E+02	6.44E+02	5.98E+02	6.71E+02	6.06E+02
Pu-242	2.49E+02	2.35E+02	2.33E+02	2.33E+02	2.41E+02
Pu-243	8.77E-02	9.74E-02	9.29E-02	9.78E-02	9.88E-02
Pu-244	8.99E-03	1.52E-02	1.40E-02	1.54E-02	9.72E-03
Am-241	1.17E+01	1.31E+01	1.20E+01	1.37E+01	1.22E+01
Am-242	5.06E-02	4.90E-02	4.73E-02	5.00E-02	4.36E-02
Am-242m	2.36E-01	1.82E-01	1.24E-01	1.96E-01	2.44E-01
Am-243	4.48E+01	4.94E+01	4.62E+01	4.97E+01	5.08E+01
Am-244	5.84E-02	4.05E-03	3.69E-03	4.12E-03	6.18E-02
Cm-242	5.60E+00	5.26E+00	5.03E+00	5.36E+00	4.63E+00
Cm-243	1.15E-01	1.08E-01	1.00E-01	1.12E-01	1.16E-01
Cm-244	1.36E+01	1.49E+01	1.32E+01	1.53E+01	1.44E+01
Cm-245	6.94E-01	8.38E-01	7.26E-01	8.99E-01	5.37E-01
Cm-246	6.05E-02	7.03E-02	6.39E-02	7.19E-02	4.70E-02
Cm-247	6.52E-04	7.50E-04	6.49E-04	7.94E-04	4.45E-04
Cm-248	3.41E-05	4.14E-05	3.47E-05	4.44E-05	2.40E-05
Bk-249	3.42E-07	4.20E-07	3.25E-07	4.74E-07	2.44E-07
Cf-249	3.09E-08	3.82E-08	2.78E-08	4.37E-08	2.17E-08
Cf-250	1.84E-07	1.73E-07	1.46E-07	1.86E-07	5.54E-08
Cf-251	4.03E-08	6.67E-08	5.26E-08	7.39E-08	2.96E-08
Cf-252	2.07E-08	3.33E-08	2.73E-08	3.53E-08	1.53E-08
Total	4.53E+05	4.53E+05	4.53E+05	4.53E+05	4.53E+05

Table 5. Calculated HM masses [g] in UOX assembly at discharge.

Calculated Fission Product masses at EoL are listed in Table 6.

	APOLLO2	NEWT	Serpent	KENO-VI	Origen-Arp
Kr-83	1.87E+01	1.92E+01	1.94E+01	1.92E+01	1.92E+01
Rh-103	2.05E+02	2.05E+02	2.03E+02	2.05E+02	2.04E+02
Rh-105	8.45E-01	7.66E-01	7.91E-01	7.67E-01	7.55E-01
Ag-109	3.67E+01	3.76E+01	3.70E+01	3.76E+01	3.67E+01
I-135	3.29E-01	3.36E-01	3.38E-01	3.36E-01	3.38E-01
Xe-131	1.92E+02	2.00E+02	2.01E+02	2.00E+02	1.96E+02
Xe-135	8.68E-02	9.22E-02	8.47E-02	9.26E-02	8.83E-02
Cs-133	5.15E+02	5.24E+02	5.22E+02	5.24E+02	5.28E+02
Cs-134	6.13E+01	6.15E+01	6.08E+01	6.15E+01	5.57E+01
Cs-135	1.26E+02	1.31E+02	1.23E+02	1.30E+02	1.33E+02
Cs-137	5.67E+02	5.72E+02	5.74E+02	5.72E+02	5.78E+02
Ba-137m	-	8.82E-05	8.82E-05	8.82E-05	8.91E-05
Ba-140	-	1.42E+01	1.43E+01	1.42E+01	1.43E+01
La-140	1.93E+00	1.92E+00	1.94E+00	1.92E+00	1.94E+00
Nd-143	3.58E+02	3.63E+02	3.58E+02	3.63E+02	3.62E+02
Nd-145	3.15E+02	3.10E+02	3.11E+02	3.10E+02	3.15E+02
Nd-148	1.77E+02	1.75E+02	1.74E+02	1.75E+02	1.73E+02
Pm-147	9.53E+01	9.22E+01	9.38E+01	9.42E+01	8.95E+01
Pm-148	7.75E-01	8.02E-01	7.92E-01	7.80E-01	6.53E-01
Pm-149	8.63E-01	8.51E-01	8.66E-01	8.43E-01	9.67E-01
Sm-147	2.39E+01	2.34E+01	2.37E+01	2.37E+01	2.31E+01
Sm-149	9.70E-01	1.08E+00	9.78E-01	1.07E+00	1.13E+00
Sm-150	1.39E+02	1.38E+02	1.39E+02	1.39E+02	1.45E+02
Sm-151	5.29E+00	5.61E+00	5.09E+00	5.45E+00	7.05E+00
Sm-152	5.13E+01	5.13E+01	5.05E+01	5.02E+01	6.11E+01
Eu-153	5.43E+01	5.49E+01	5.37E+01	5.42E+01	5.38E+01
Eu-154	1.11E+01	1.14E+01	1.07E+01	1.14E+01	1.06E+01
Eu-155	3.71E+00	3.75E+00	3.84E+00	3.74E+00	2.56E+00
Eu-156	2.61E+00	2.65E+00	2.69E+00	2.64E+00	2.59E+00
Gd-155	1.81E-02	1.88E-02	1.74E-02	1.88E-02	1.32E-02
Total	2.96E+03	3.00E+03	2.99E+03	3.00E+03	3.01E+03

Table 6. Calculated FP masses [g] in UOX assembly at discharge.

The calculated masses of Heavy Metals and Fission Products after 30 years of cooling are shown in Tables 7 and 8, respectively.

	APOLLO2 Origen-S	NEWT Origen-S	Serpent Origen-S	KENO-VI Origen-S	Origen-Arp
U-234	9.48E+01	9.69E+01	9.57E+01	9.57E+01	9.55E+01
U-235	3.70E+03	3.84E+03	3.65E+03	3.83E+03	3.66E+03
U-236	1.80E+03	1.81E+03	1.82E+03	1.81E+03	1.83E+03
U-237	4.60E-06	4.69E-06	4.35E-06	4.71E-06	4.31E-06
U-238	4.43E+05	4.42E+05	4.43E+05	4.42E+05	4.43E+05
Np-237	1.94E+02	2.06E+02	2.03E+02	2.06E+02	2.08E+02
Pu-238	5.08E+01	5.00E+01	4.79E+01	4.79E+01	5.17E+01
Pu-239	2.57E+03	2.71E+03	2.51E+03	2.73E+03	2.58E+03
Pu-240	1.10E+03	1.12E+03	1.11E+03	1.12E+03	1.11E+03
Pu-241	1.48E+02	1.50E+02	1.40E+02	1.51E+02	1.42E+02
Pu-242	2.49E+02	2.35E+02	2.33E+02	2.34E+02	2.41E+02
Am-241	4.82E+02	4.92E+02	4.57E+02	4.95E+02	4.62E+02
Am-242	2.63E-06	2.03E-06	1.34E-06	2.04E-06	2.72E-06
Am-242M	2.04E-01	1.57E-01	1.04E-01	1.58E-01	2.11E-01
Am-243	4.48E+01	4.93E+01	4.62E+01	4.85E+01	5.07E+01
Am-244	0.00E+00	0.00E+00	0.00E+00	0.00E+00	0.00E+00
Cm-244	4.32E+00	4.71E+00	4.18E+00	2.21E+00	4.59E+00
Cm-245	6.92E-01	8.36E-01	7.24E-01	3.99E-01	5.36E-01
Cf-251	3.94E-08	6.52E-08	5.18E-08	6.20E-08	2.89E-08
Cf-252	7.98E-12	1.28E-11	1.05E-11	1.20E-11	5.87E-12
Total	4.53E+05	4.53E+05	4.53E+05	4.53E+05	4.53E+05

Table 7. Calculated HM masses [g] in UOX assembly after 30 years.

	APOLLO2 Origen-S	NEWT Origen-S	Serpent Origen-S	KENO-VI Origen-S	Origen-Arp
Sr-90	1.19E+02	1.21E+02	1.22E+02	1.21E+02	1.20E+02
Y-90	3.01E-02	3.07E-02	3.10E-02	3.08E-02	3.12E-02
Cs-137	2.84E+02	2.86E+02	2.87E+02	2.86E+02	2.89E+02
Ba-137m	4.34E-05	4.37E-05	4.39E-05	4.37E-05	4.41E-05
Sm-154	1.79E+01	1.79E+01	1.77E+01	1.79E+01	1.72E+01
Eu-153	5.43E+01	5.49E+01	5.37E+01	5.42E+01	5.45E+01
Eu-154	9.89E-01	1.02E+00	9.53E-01	1.01E+00	9.38E-01
Eu-155	4.67E-02	4.72E-02	4.83E-02	4.70E-02	3.01E-02
Total	4.76E+02	4.81E+02	4.82E+02	4.81E+02	4.82E+02

Table 8. Calculated FP masses [g] in UOX assembly after 30 years.

Calculated 30-year gamma release rates and contributions from each energy group for each are listed in Table 9.

E _{low} [MeV]	E _{high} [MeV]	APOLLO2 Origen-S		NEWT Origen-S		Serpent Origen-S		KENO-VI Origen-S		Origen-ARP	
		Gamma release rate [photons/s]	Percent of total gammas	Gamma release rate [photons/s]	Percent of total gammas	Gamma release rate [photons/s]	Percent of total gammas	Gamma release rate [photons/s]	Percent of total gammas	Gamma release rate [photons/s]	Percent of total gammas
0.00	0.02	5.19E+14	2.66E-01	5.29E+14	2.68E-01	5.31E+14	2.68E-01	5.28E+14	2.67E-01	5.38E+14	2.69E-01
0.02	0.03	1.01E+14	5.19E-02	1.03E+14	5.22E-02	1.04E+14	5.24E-02	1.03E+14	5.22E-02	1.05E+14	5.26E-02
0.03	0.05	1.34E+14	6.86E-02	1.36E+14	6.87E-02	1.36E+14	6.88E-02	1.36E+14	6.87E-02	1.38E+14	6.88E-02
0.05	0.07	1.04E+14	5.35E-02	1.06E+14	5.39E-02	1.05E+14	5.32E-02	1.07E+14	5.39E-02	1.07E+14	5.33E-02
0.07	0.10	5.52E+13	2.84E-02	5.64E+13	2.85E-02	5.69E+13	2.87E-02	5.64E+13	2.86E-02	5.74E+13	2.87E-02
0.10	0.15	4.81E+13	2.47E-02	4.92E+13	2.49E-02	4.93E+13	2.49E-02	4.91E+13	2.49E-02	4.96E+13	2.48E-02
0.15	0.30	4.78E+13	2.46E-02	4.89E+13	2.47E-02	4.92E+13	2.48E-02	4.89E+13	2.48E-02	4.96E+13	2.48E-02
0.30	0.45	2.00E+13	1.03E-02	2.05E+13	1.04E-02	2.06E+13	1.04E-02	2.05E+13	1.04E-02	2.08E+13	1.04E-02
0.45	0.70	9.03E+14	4.64E-01	9.11E+14	4.61E-01	9.14E+14	4.61E-01	9.11E+14	4.61E-01	9.19E+14	4.60E-01
0.70	1.00	9.15E+12	4.70E-03	9.38E+12	4.75E-03	9.08E+12	4.58E-03	9.36E+12	4.74E-03	9.02E+12	4.51E-03
1.00	1.50	6.14E+12	3.15E-03	6.30E+12	3.19E-03	6.00E+12	3.03E-03	6.28E+12	3.18E-03	5.94E+12	2.97E-03
1.50	2.00	3.07E+11	1.58E-04	3.15E+11	1.59E-04	3.03E+11	1.53E-04	3.14E+11	1.59E-04	3.01E+11	1.51E-04
2.00	2.50	2.06E+09	1.06E-06	2.11E+09	1.07E-06	2.12E+09	1.07E-06	2.10E+09	1.06E-06	2.13E+09	1.07E-06
2.50	3.00	1.05E+08	5.38E-08	1.60E+08	8.11E-08	8.16E+06	4.12E-09	1.57E+08	7.97E-08	8.44E+07	4.22E-08
3.00	4.00	5.30E+06	2.72E-09	5.76E+06	2.92E-09	5.12E+06	2.58E-09	2.83E+06	1.44E-09	5.59E+06	2.80E-09
4.00	6.00	2.27E+06	1.16E-09	2.46E+06	1.25E-09	2.19E+06	1.11E-09	1.21E+06	6.12E-10	2.39E+06	1.20E-09
6.00	8.00	2.61E+05	1.34E-10	2.84E+05	1.43E-10	2.52E+05	1.27E-10	1.39E+05	7.03E-11	2.75E+05	1.38E-10
8.00	11.00	3.00E+04	1.54E-11	3.26E+04	1.65E-11	2.90E+04	1.46E-11	1.60E+04	8.08E-12	3.17E+04	1.58E-11
Total		1.95E+15	1.00E+00	1.98E+15	1.00E+00	1.98E+15	1.00E+00	1.97E+15	1.00E+00	2.00E+15	1.00E+00

Table 9. Calculated 30-year gamma release rates and contributions from each energy group for UOX assembly.

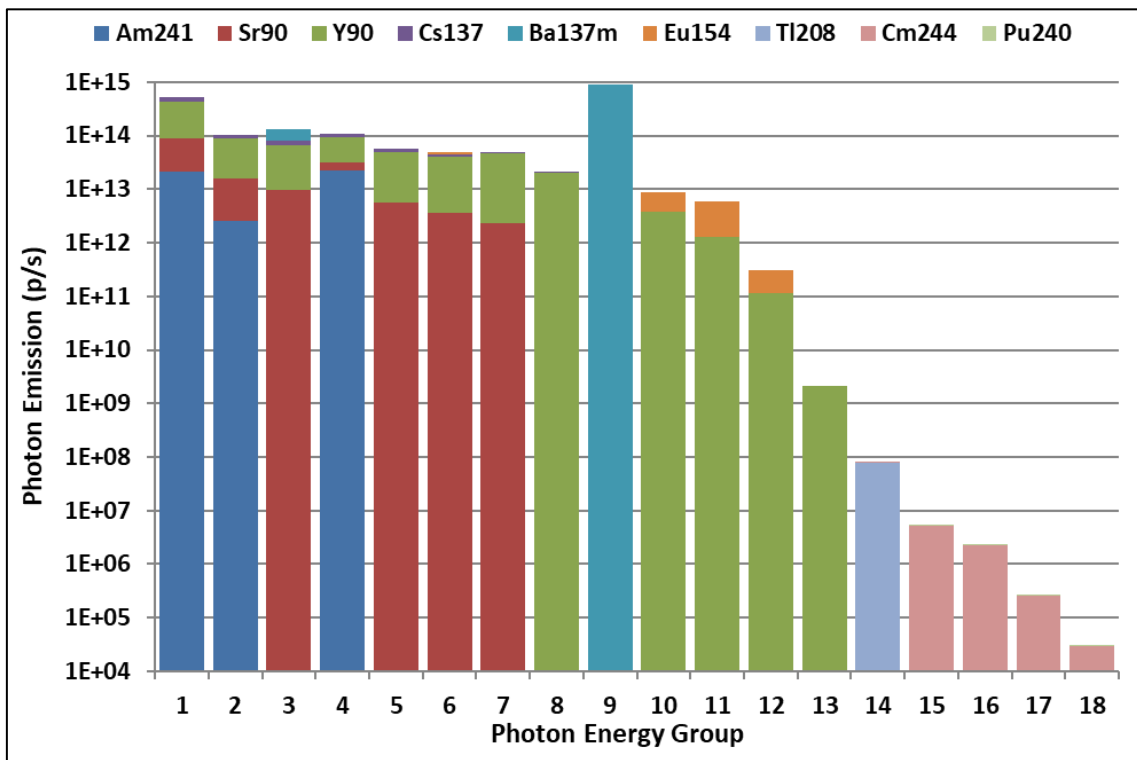


Figure 4. Contributors to the primary photon emission.

For each energy group, the most relevant isotopes in terms of photon emission according to the strategy 1 are shown in Figure 4. From this it can be concluded that these isotopes, in descending order of importance, are: Ba137m, Y90, Cs137, Sr90, Am241, Eu154, Tl208, Cm244, and Pu240. In this regard, it is worth noting that the isotope Tl208, that is the most important contributor of the group 14, was not included in the Benchmark specifications.

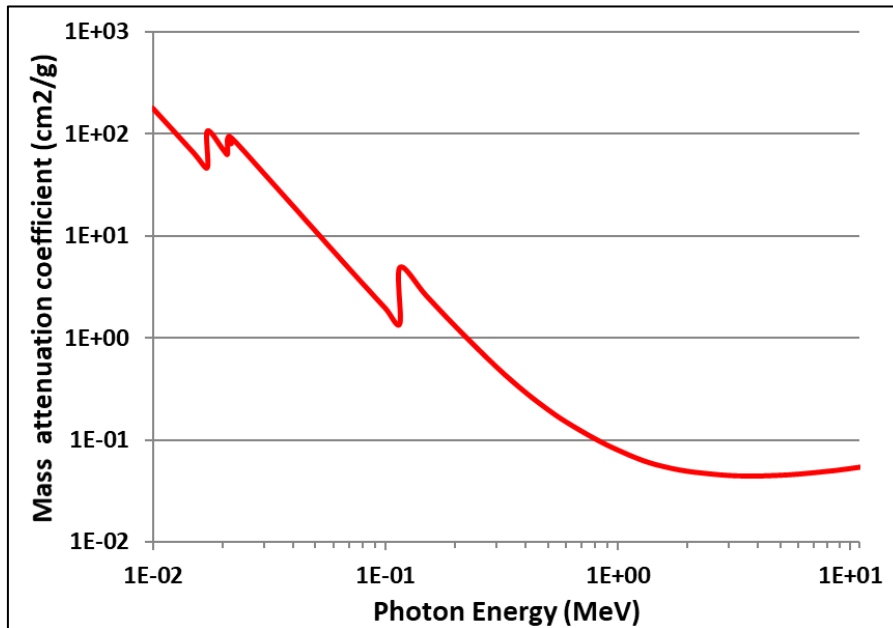


Figure 5. Mass attenuation coefficient of U.

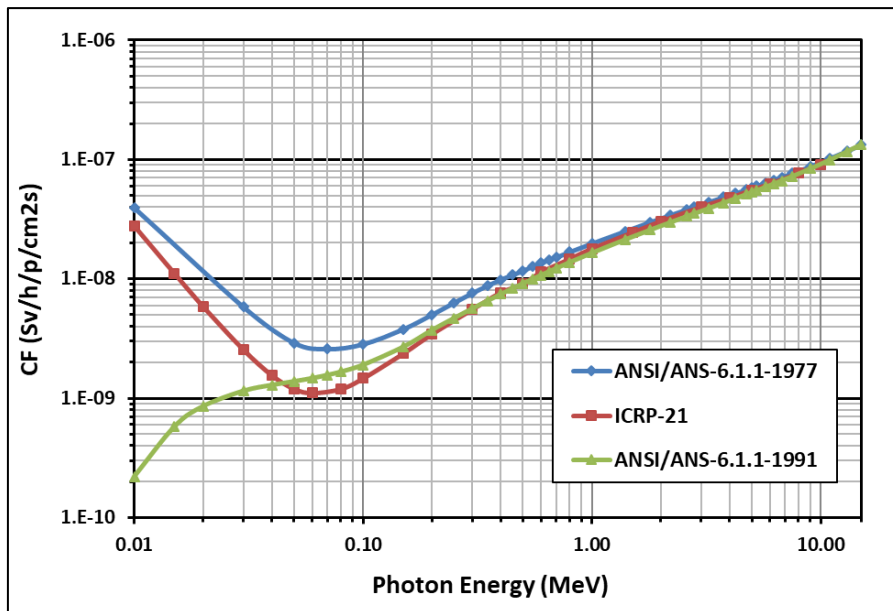


Figure 6. ANSI/ANS-6.1.1 conversion factors.

However, it should be noted that these isotopes are not necessarily the most important also in terms of gamma dose rate. In fact, the gamma dose rate also depends on two non-proportional contributions, such as the photon attenuation due mostly to the fuel matrix (in Figure 5 the mass attenuation coefficient of U¹ is shown) and the flux-to-dose conversion (in Figure 6 three conversion factor models are depicted), both strongly variable with energy. Combining these contributions, the most relevant isotopes in terms of gamma dose rate are those that emit above 0.4 MeV.

The results of the gamma dose rate at 1 m from the midpoint after 30 years of decay are shown in Table 10.

Conversion factors	APOLLO2 Origen-S MCNPX	NEWT Origen-S MCNPX	Serpent Origen-S MCNPX	KENO-VI Origen-S MCNPX	Origen-ARP MCNPX	Average
ANSI/ANS-6.1.1-1977	5.25	5.34	5.21	5.22	5.20	5.24
ANSI/ANS-6.1.1-1991	4.13	4.21	4.11	4.11	4.09	4.13
ICRP60	-	-	-	-	3.86	3.86

Table 10. Calculated 30-year gamma dose rates [Sv/h] at 1 m from the midpoint for UOX FA.

The following can be noted:

- the five calculation strategies of Table 4 show a very good agreement in each phase, i.e. nuclide inventory, gamma source and gamma dose rate;
- the gamma dose rates calculated with the ANSI/ANS-6.1.1-1991 conversion factor are about 20% lower than those calculated with the 1977 version;
- ICRP60 standard provides a value, calculated only according to the strategy 5, which is 5.6% and 26% lower than those calculated with the ANSI/ANS-6.1.1-1991 and ANSI/ANS-6.1.1-1977 conversion factors, respectively;
- Bremsstrahlung of the secondary electrons is slightly relevant.

Compared to the dose rates at 1 m from the center of FA in perpendicular direction estimated by [Llyod, 1994] for two PWR UOX FAs irradiated up to 30000 and 35000 MWd/MTU after a cooling time of 30 yr, 13.0 and 15.2 Sv/h respectively, these values are between 2 and 3 times lower.

With regard to the values obtained with the ANSI/ANS-6.1.1-1991 conversion factor according to the strategy 5, it can be seen in Table 11 that 98.8% of total gamma dose rate is due to three energy groups, namely 9, 10, and 11 and 93.9% to the only group 9 i.e. to the photon contribution of Ba137m. Y90 and Eu154 contribute almost 5% to the total dose rate, a small but not negligible contribution. It is therefore confirmed that, in this study, the most important energy range for the dose rate calculation is between 0.45 and 1.5 MeV.

¹ <https://www.nist.gov/pml/x-ray-mass-attenuation-coefficients>

Photon energy group	Energy range [MeV]	Dose rate (Sv/h)	Dose rate % wrt Total	Nuclides
9	0.45-0.70	3.84	93.9	Ba137m, (Cs137)
10	0.70-1.00	0.11	2.7	Y90, Eu154
11	1.00-1.50	0.09	2.2	Y90, Eu154
9+10+11	0.45-1.50	4.04	98.8	-
All groups	0.00-11.00	4.09	100	-

Table 11. Photon contribution to dose rate.

The values for both conversion factors of the gamma dose rates at 1 m from the midplane for the UOX FA after a period of decay of 3.7 y are shown in Table 12. These values are calculated according to the strategy 5. The photon source, calculated with the 18 energy group structure, is equal to $9.45E+15$ photons/s.

Conversion factors	Origen-ARP MCNPX
ANSI/ANS-6.1.1-1977	32.22
ANSI/ANS-6.1.1-1991	25.77

Table 12. Calculated 3.7-year gamma dose rates [Sv/h] at 1 m from the midpoint for UOX FA.

2.3.2 Results for MOX PWR fuel assembly

Calculated Heavy Metal masses at EoL are shown in Table 13.

	APOLLO2	NEWT	Serpent	KENO-VI	Origen-Arp
U-234	2.19E+01	2.23E+01	2.21E+01	2.23E+01	2.11E+01
U-235	4.33E+02	4.29E+02	4.25E+02	4.31E+02	4.38E+02
U-236	1.31E+02	1.32E+02	1.33E+02	1.32E+02	1.31E+02
U-237	1.13E+00	1.19E+00	1.21E+00	1.19E+00	1.15E+00
U-238	3.97E+05	3.96E+05	3.96E+05	3.96E+05	3.96E+05
Np-236	9.77E-04	2.93E-04	1.38E-03	2.95E-04	3.66E-04
Np-236M	-	5.37E-06	1.69E-09	5.38E-06	1.95E-06
Np-237	9.25E+01	1.00E+02	1.02E+02	1.00E+02	9.44E+01
Np-238	2.10E-01	2.18E-01	2.19E-01	2.18E-01	2.11E-01
Np-239	3.82E+01	3.81E+01	3.93E+01	3.82E+01	3.88E+01
Pu-236	4.76E-04	1.54E-03	8.27E-04	1.55E-03	1.10E-03
Pu-237	3.24E-03	4.19E-03	4.24E-03	4.21E-03	3.72E-03
Pu-238	1.03E+03	1.02E+03	1.02E+03	1.02E+03	1.00E+03
Pu-239	9.20E+03	9.30E+03	9.43E+03	9.35E+03	9.77E+03
Pu-240	8.18E+03	8.21E+03	8.23E+03	8.17E+03	8.10E+03
Pu-241	4.69E+03	4.68E+03	4.73E+03	4.71E+03	4.83E+03
Pu-242	3.84E+03	3.64E+03	3.59E+03	3.63E+03	3.65E+03
Pu-243	4.20E-01	4.53E-01	4.63E-01	4.56E-01	4.67E-01
Pu-244	1.14E-01	4.11E-01	4.24E-01	4.14E-01	1.28E-01
Am-241	4.14E+02	4.68E+02	4.75E+02	4.71E+02	4.71E+02
Am-242	5.97E-01	5.97E-01	6.12E-01	5.99E-01	5.60E-01
Am-242M	1.32E+01	1.06E+01	8.04E+00	1.08E+01	1.57E+01
Am-243	9.06E+02	1.00E+03	1.03E+03	1.01E+03	1.03E+03
Am-244	6.11E-01	4.16E-02	4.24E-02	4.19E-02	6.97E-01
Cm-242	1.14E+02	1.13E+02	1.16E+02	1.13E+02	1.05E+02
Cm-243	6.06E+00	5.84E+00	6.13E+00	5.87E+00	6.32E+00
Cm-244	6.23E+02	6.81E+02	6.95E+02	6.85E+02	7.32E+02
Cm-245	8.01E+01	9.82E+01	1.02E+02	9.94E+01	9.47E+01
Cm-246	7.42E+00	9.28E+00	9.47E+00	9.30E+00	8.35E+00
Cm-247	1.89E-01	2.35E-01	2.33E-01	2.36E-01	1.99E-01
Cm-248	1.48E-02	2.12E-02	2.04E-02	2.12E-02	1.41E-02
Bk-249	3.38E-04	4.59E-04	4.73E-04	4.61E-04	3.08E-04
Cf-249	9.38E-05	1.30E-04	1.31E-04	1.31E-04	8.86E-05
Cf-250	1.56E-04	1.39E-04	1.44E-04	1.39E-04	7.51E-05
Cf-251	3.04E-05	7.78E-05	7.83E-05	7.80E-05	6.37E-05
Cf-252	1.15E-05	3.03E-05	2.92E-05	3.00E-05	2.26E-05
Total	4.26E+05	4.26E+05	4.26E+05	4.26E+05	4.26E+05

Table 13. Calculated Heavy Metal masses [g] in MOX assembly at discharge.

Calculated Fission Product masses at EoL are listed in Table 14.

	APOLLO2	NEWT	Serpent	KENO-VI	Origen-Arp
Kr-83	2.13E+01	2.28E+01	2.33E+01	2.29E+01	2.24E+01
Rh-103	5.49E+02	5.56E+02	5.65E+02	5.56E+02	5.30E+02
Ag-109	1.43E+02	1.43E+02	1.44E+02	1.43E+02	1.33E+02
I-135	2.76E-01	2.78E-01	2.81E-01	2.78E-01	2.70E-01
Xe-131	3.38E+02	3.59E+02	3.61E+02	3.58E+02	3.22E+02
Xe-135	2.15E-01	2.18E-01	2.21E-01	2.20E-01	2.26E-01
Cs-133	8.56E+02	8.69E+02	8.71E+02	8.69E+02	8.54E+02
Cs-134	1.22E+02	1.21E+02	1.24E+02	1.21E+02	1.06E+02
Cs-135	6.40E+02	6.59E+02	6.64E+02	6.62E+02	6.78E+02
Cs-137	9.75E+02	9.92E+02	1.00E+03	9.92E+02	9.96E+02
Ba-137m	-	1.53E-04	1.53E-04	1.53E-04	1.53E-04
Ba-140	-	1.12E+01	1.13E+01	1.12E+01	1.14E+01
La-140	1.54E+00	1.51E+00	1.52E+00	1.51E+00	1.54E+00
Nd-143	6.07E+02	6.10E+02	6.16E+02	6.10E+02	6.08E+02
Nd-145	4.60E+02	4.57E+02	4.60E+02	4.57E+02	4.51E+02
Nd-148	6.54E-01	3.01E+02	3.03E+02	3.01E+02	2.94E+02
Pm-147	1.16E+02	1.12E+02	1.13E+02	1.12E+02	1.07E+02
Pm-148	6.54E-01	6.50E-01	6.55E-01	6.50E-01	5.79E-01
Pm-149	6.90E-01	6.60E-01	6.73E-01	6.60E-01	6.91E-01
Sm-147	5.82E+01	5.79E+01	5.76E+01	5.79E+01	5.62E+01
Sm-149	3.73E+00	3.89E+00	3.96E+00	3.95E+00	4.47E+00
Sm-150	2.50E+02	2.40E+02	2.50E+02	2.40E+02	2.46E+02
Sm-151	2.03E+01	2.08E+01	2.04E+01	2.10E+01	2.69E+01
Sm-152	9.29E+01	9.15E+01	9.10E+01	9.14E+01	9.46E+01
Eu-153	1.25E+02	1.30E+02	1.27E+02	1.30E+02	1.26E+02
Eu-154	4.52E+01	4.65E+01	4.65E+01	4.66E+01	4.61E+01
Eu-155	1.05E+01	1.09E+01	1.14E+01	1.09E+01	7.34E+00
Eu-156	3.17E+00	3.23E+00	3.24E+00	3.22E+00	3.10E+00
Gd-155	2.79E-01	2.82E-01	2.99E-01	2.87E-01	2.44E-01
Total	5.44E+03	5.82E+03	5.87E+03	5.82E+03	5.73E+03

Table 14. Calculated Fission Product masses [g] in MOX assembly at discharge.

The calculated masses of Heavy Metals and Fission Products after 30 years of cooling are shown in Tables 15 and 16, respectively.

	APOLLO2 Origen-S	NEWT Origen-S	Serpent Origen-S	KENO-VI Origen-S	Origen-Arp
U-234	2.59E+02	2.57E+02	2.57E+02	2.52E+02	2.51E+02
U-235	4.41E+02	4.37E+02	4.33E+02	4.46E+02	4.46E+02
U-236	1.57E+02	1.58E+02	1.59E+02	2.00E+02	1.57E+02
U-237	3.41E-05	3.41E-05	3.45E-05	3.51E-05	3.43E-05
U-238	3.97E+05	3.96E+05	3.96E+05	3.96E+05	3.96E+05
Np-237	2.16E+02	2.26E+02	2.29E+02	1.29E+02	2.23E+02
Pu-238	9.03E+02	8.94E+02	8.97E+02	8.76E+02	8.76E+02
Pu-239	9.24E+03	9.34E+03	9.47E+03	9.80E+03	9.81E+03
Pu-240	8.57E+03	8.64E+03	8.67E+03	8.56E+03	8.56E+03
Pu-241	1.09E+03	1.09E+03	1.10E+03	1.13E+03	1.13E+03
Pu-242	3.84E+03	3.64E+03	3.59E+03	3.65E+03	3.65E+03
Am-241	3.89E+03	3.93E+03	3.98E+03	4.04E+03	4.03E+03
Am-242	1.47E-04	1.18E-04	8.95E-05	1.75E-04	1.75E-04
Am-242m	1.14E+01	9.15E+00	6.94E+00	1.36E+01	1.36E+01
Am-243	9.04E+02	9.98E+02	1.03E+03	5.78E-01	1.03E+03
Am-244	0.00E+00	0.00E+00	0.00E+00	0.00E+00	0.00E+00
Cm-244	1.98E+02	2.16E+02	2.20E+02	2.32E+02	2.32E+02
Cm-245	7.99E+01	9.80E+01	1.02E+02	9.45E+01	9.45E+01
Cf-251	2.97E-05	7.60E-05	7.66E-05	6.22E-05	6.22E-05
Cf-252	4.43E-09	1.17E-08	1.12E-08	8.71E-09	8.71E-09
Total	4.27E+05	4.26E+05	4.26E+05	4.25E+05	4.26E+05

Table 15. Calculated Heavy Metal masses [g] in MOX assembly after 30 years.

	APOLLO2 Origen-S	NEWT Origen-S	Serpent Origen-S	KENO-VI Origen-S	Origen-Arp
Sr-90	9.74E+01	1.01E+02	1.02E+02	1.01E+02	9.78E+01
Y-90	2.47E-02	2.56E-02	2.59E-02	2.56E-02	2.54E-02
Cs-137	4.88E+02	4.97E+02	5.01E+02	4.97E+02	4.98E+02
Ba-137	4.87E+02	5.43E+02	5.47E+02	5.43E+02	5.46E+02
Ba-137m	7.46E-05	7.59E-05	7.66E-05	7.59E-05	7.60E-05
Sm-154	5.29E+01	5.25E+01	5.29E+01	5.25E+01	5.17E+01
Eu-153	1.25E+02	1.30E+02	1.27E+02	1.30E+02	1.27E+02
Eu-154	4.03E+00	4.14E+00	4.14E+00	4.16E+00	4.09E+00
Eu-155	1.32E-01	1.37E-01	1.43E-01	1.37E-01	8.64E-02
Total	1.25E+03	1.33E+03	1.34E+03	1.33E+03	1.32E+03

Table 16. Calculated Fission Product masses [g] in MOX assembly after 30 years.

Calculated 30-year gamma release rates and contributions from each energy group are listed in Table 17.

E _{low} [MeV]	E _{high} [MeV]	APOLLO2 Origen-S		NEWT Origen-S		Serpent Origen-S		KENO-VI Origen-S		Origen-ARP	
		Gamma release rate [photons/s]	Percent of total gammas	Gamma release rate [photons/s]	Percent of total gammas	Gamma release rate [photons/s]	Percent of total gammas	Gamma release rate [photons/s]	Percent of total gammas	Gamma release rate [photons/s]	Percent of total gammas
0.00	0.02	8.83E+14	2.73E-01	9.07E+14	2.74E-01	9.16E+14	2.74E-01	1.20E+15	3.19E-01	9.15E+14	2.75E-01
0.02	0.03	1.30E+14	4.01E-02	1.33E+14	4.03E-02	1.35E+14	4.03E-02	1.50E+14	3.98E-02	1.33E+14	4.01E-02
0.03	0.05	1.80E+14	5.56E-02	1.84E+14	5.57E-02	1.86E+14	5.57E-02	1.84E+14	4.90E-02	1.84E+14	5.53E-02
0.05	0.07	2.63E+14	8.13E-02	2.68E+14	8.09E-02	2.71E+14	8.10E-02	2.73E+14	7.25E-02	2.72E+14	8.19E-02
0.07	0.10	5.73E+13	1.77E-02	5.95E+13	1.80E-02	6.03E+13	1.80E-02	1.39E+14	3.69E-02	5.89E+13	1.77E-02
0.10	0.15	6.29E+13	1.94E-02	6.50E+13	1.97E-02	6.56E+13	1.97E-02	8.93E+13	2.37E-02	6.46E+13	1.94E-02
0.15	0.30	4.86E+13	1.50E-02	5.04E+13	1.52E-02	5.10E+13	1.53E-02	8.45E+13	2.24E-02	5.00E+13	1.50E-02
0.30	0.45	1.75E+13	5.40E-03	1.81E+13	5.48E-03	1.83E+13	5.49E-03	1.81E+13	4.80E-02	1.79E+13	5.38E-03
0.45	0.70	1.55E+15	4.78E-01	1.58E+15	4.76E-01	1.59E+15	4.76E-01	1.58E+15	4.19E-01	1.58E+15	4.76E-01
0.70	1.00	2.48E+13	7.68E-03	2.56E+13	7.73E-03	2.56E+13	7.66E-03	2.64E+13	7.02E-03	2.53E+13	7.60E-03
1.00	1.50	2.09E+13	6.45E-03	2.15E+13	6.49E-03	2.15E+13	6.43E-03	2.16E+13	5.73E-03	2.13E+13	6.39E-03
1.50	2.00	8.95E+11	2.77E-04	9.21E+11	2.78E-04	9.22E+11	2.76E-04	9.93E+11	2.64E-04	9.12E+11	2.74E-04
2.00	2.50	2.14E+09	6.61E-07	2.25E+09	6.79E-07	2.28E+09	6.81E-07	2.28E+09	6.07E-07	2.25E+09	6.78E-07
2.50	3.00	3.69E+08	1.14E-07	6.28E+08	1.90E-07	4.77E+08	1.43E-07	1.44E+12	3.84E-04	5.51E+08	1.66E-07
3.00	4.00	2.37E+08	7.34E-08	2.60E+08	7.86E-08	2.65E+08	7.93E-08	4.07E+08	1.08E-07	2.78E+08	8.36E-08
4.00	6.00	1.02E+08	3.15E-08	1.12E+08	3.37E-08	1.14E+08	3.40E-08	1.19E+08	3.17E-08	1.19E+08	3.59E-08
6.00	8.00	1.17E+07	3.62E-09	1.28E+07	3.88E-09	1.31E+07	3.92E-09	1.37E+07	3.65E-09	1.37E+07	4.13E-09
8.00	11.00	1.35E+06	4.17E-10	1.48E+06	4.46E-10	1.51E+06	4.51E-10	1.58E+06	4.20E-10	1.58E+06	4.75E-10
Total		3.24E+15	1.00E+00	3.31E+15	1.00E+00	3.34E+15	1.00E+00	3.76E+15	1.00E+00	3.32E+15	1.00E+00

Table 17. Calculated 30-year gamma release rates and contributions from each energy group for MOX FA.

The results of the gamma dose rate at 1 m from the midpoint after 30 years of decay are shown in Table 18. For both ANSI conversion factors, a very good agreement can be observed between the values obtained with the five calculation strategies. The values for the ANSI/ANS-6.1.1-1991 conversion factor are about 21% lower than those for the 1977 version, regardless of the strategy used.

Conversion factors	APOLLO2 Origen-S MCNPX	NEWT Origen-S MCNPX	Serpent Origen-S MCNPX	KENO-VI Origen-S MCNPX	Origen-ARP MCNPX	Average
ANSI/ANS-6.1.1-1977	11.40	11.62	11.72	11.75	11.65	11.63
ANSI/ANS-6.1.1-1991	9.01	9.18	9.26	9.30	9.21	9.19

Table 18. Calculated 30-year gamma dose rates [Sv/h] at 1 m from the midpoint for MOX FA.

2.4 Sensitivity analysis

To assess the impact of some calculation options on gamma dose rate, a sensitivity analysis is performed. In particular, this section is focused on the impact of the detector size and shape, type of tally and energy group structure. For this purpose, the same isotope concentrations at discharge of the UOX fuel assembly are taken into account. Origen-ARP and MCNPX are used according to the strategy 5. Unless otherwise stated, the gamma source of 2.00E+15 photons/s is considered. 1E+08 primary photons are run.

Concerning the detector size and shape, two configurations are compared to 20x20x0.5 cm³ rectangular box of the reference case:

- ✓ 30x30x5 cm³ rectangular box;
- ✓ sphere with a radius of 10.2418 cm.

All configurations are centered on a point at 100 cm from the axial midpoint and 182.88 cm from the bottom of the active length. As shown in Table 19, the percentage variations of these configurations with respect to the gamma dose rate values of the reference case are widely lower than the statistical uncertainties of the calculations and therefore negligible. This is confirmed for both conversion factors.

	Rectangular box (V=200 cm³)	Rectangular box (V=4500 cm³)	Sphere (V=4500 cm³)
Dose rate for AINSI/ANS-6.1.1-1977 [Sv/h]	5.20 ±3.11%	5.24 ±2.04%	5.23 ±3.28%
Relative difference [%]	[-]	0.80	0.57
Dose rate for AINSI/ANS-6.1.1-1991 [Sv/h]	4.09 ±3.12%	4.12 ±2.03%	4.11 ±3.28%
Relative difference [%]	[-]	0.68	0.58

Table 19. Impact of detector size and shape.

As a further comparison, two types of tallies are compared in terms of gamma dose rate: f4 (cell flux tally) of the reference case and f5 (point flux tally). In both cases, the detector is centered at 100 cm from the axial midpoint and 182.88 cm from the bottom of the active length. For tallies f5, the radius of the sphere of exclusion is set to 20 cm. In Table 20 a small but not completely negligible discrepancy between two calculations can be observed.

	Tally f4	Tally f5
Dose rate [Sv/h] (AINSI/ANS-1977)	5.20 ±3.11%	5.10 ±0.30%
Relative difference [%]	[-]	-1.99
Dose rate [Sv/h] (AINSI/ANS-1991)	4.09 ±3.12%	4.00 ±0.30%
Relative difference [%]	[-]	-2.10

Table 20. Impact of type of tally.

Finally, the 18 group structure of the reference case is compared to the other two structures with 19 and 62 energy groups contained in Appendix II. The photon release rates in the three cases, along with the values of gamma dose rates for both AINSI/ANS conversion factors and the percentage variations related to the reference case values are given in Table 21. These results highlight how different structures can cause significant discrepancies in photon release rates and consequently in dose rates. Unfortunately, there is not a direct way to compare different release rates obtained with different group structures. Despite this, the choice of the energy group structure is a crucial aspect for this type of calculation.

	18 group	19 group	62 group
Photon release rate [p/s]	2.00E+15	1.71E+15	1.32E+15
Dose rate [Sv/h] (AINSI/ANS-1977)	5.20	5.62	6.09
Relative difference [%]	[-]	+8.08	+17.12
Dose rate [Sv/h] (AINSI/ANS-1991)	4.09	4.46	4.84
Relative difference [%]	[-]	9.05	+18.34

Table 21. Impact of energy group structure.

3. Validation part

3.1 Computational model

In this part of the benchmark, the gamma dose rate measurements performed on a Westinghouse 15x15-21LOPAR UOX fuel assembly are used to validate the calculation strategy developed in the previous part. The fuel assembly number D04 was irradiated from December 1974 to November 1977 in the Turkey Point Unit 3, a Westinghouse PWR design with nominal power of 693 MWe (2300 MWth) operated by Florida Power and Light. The gamma dose rates of the irradiated assembly D04 were measured by thermoluminescent dosimeters (TLD) during the course of nondestructive assay tests within a hot cell at Battelle-Columbus Laboratories. All relevant data about D04 FA, including the estimated average burnup and the three irradiation cycles from which it is possible to derive both irradiation time and intermediate decay periods, are shown in Table 22 [Nichol, 1997; Willingham, 1981]. It is worth noting that the value of the specific power of Table 22, i.e. 31.203 W/g, is not consistent with the values of average burnup and irradiation time from which it would be calculated. In place of it, the value of 33.41 W/g is used in the following.

Parameter	Value
Dimensions [cm]	21.4x21.4
Element pitch [cm]	21.5
Half water blade [cm]	0.05
Cell pitch [cm]	1.427
Fuel Radius [cm]	0.4492
Gap thickness [cm]	0.025
Clad thickness [cm]	0.0618
Active fuel height [cm]	365.76
Total UO ₂ volume [cm ³]	52710.77
UO ₂ mass [kg]	518.32
U mass [kg]	456.9
²³⁵ U enrichment [wt%]	2.55
Theoretical density [g/cm ³]	10.96
Smear density (92% TD) [g/cm ³]	9.833
Clad (Zr-4) density [g/cm ³]	6.56
Fuel temperature [K]	922
Clad temperature [K]	595
Moderator temperature [K]	570
Moderator density [g/cm ³]	0.731
Start/End of Cycle 2	12/16/74 – 10/26/75
Start/End of Cycle 3	12/23/75 – 11/15/76
Start/End of Cycle 4	01/16/77 – 11/24/77
Assembly average burnup [MWd/t]	28430
Irradiation time [FPD]	851
Specific power [W/g]	31.203
Cooling Time [d]	657

Table 22. Parameters for D04 FA.

3.2 Codes and nuclear data libraries

The strategy adopted in this part is detailed in Table 23. A brief description of modeling tools and approaches used in each phase is provided below.

Phase	Strategy 5
Burnup & depletion	Origen-S
Decay & Photon source	
Photon transport	MCNPX

Table 23. Computational tools.

3.2.1 Burnup and depletion phase

Origen-S

The effective cross sections refer to the 1-grp W15x15 library prepared by ORNL using NEWT with 44-gr, LWR-optimized, micro-library based on ENDF/B-V evaluations. The water density is set to 0.731 g/cm³ according to the value of Table 22. The depletion chain includes 1946 linked nuclides. No cut-offs are used.

3.2.2 Decay and photon emission phase

ORIGEN-S

Photon emission is performed using the 18-energy group structure contained in Appendix II. Bremsstrahlung due to decay only is included. 10 decay steps are taken into account.

3.2.3 Photon transport phase

MCNPX

The photon transport and dose rate calculations are performed using the photon library mcplib04. Also in this case, it is important to note that the use of the mcplib84 [White, 2012], does not imply any difference on the gamma dose rate values. The variance reduction is of type source bias for ERG distribution (imp=2 for higher energies E>0.4 MeV). Secondary photons from (n,g) reactions are neglected. Bremsstrahlung due to secondary electrons is included with the Thick-Target Model. 5E+09 primary photons, corresponding to a maximum standard deviation on the dose of 2.2%, are used. Dose multiplier is of type DF for flux-to-dose rate conversion. Several tallies type 4 over 5x5x0.5 cm³ rectangular boxes are used. 22 detectors are placed axially and perpendicular to the FA as indicated in [Willingham, 1981]. Of these, 9 are located at 213 cm from the bottom of FA (i.e. at 183 cm from the bottom of the active length) at distances of 31, 61, 91, 122, 152, 183, 213, and 244 cm from the assembly midplane while 13 are arranged at 30.48 cm from upper flat (i.e. at 41.18 cm from assembly midplane) at distances of 0, 31, 61, 92, 122, 153, 183, 214, 244, 275, 305, 336, and 366 cm from the bottom of the active length. It is important to note that the first radial detector reported in [Willingham, 1981] is not considered in this report. However, it should be noted that its position is controversial. In fact, if in [Willingham, 1981] this is at 0 cm from the

assembly midplane, in [Davis, 1980] this is defined in contact with the assembly surface, i.e. at about 11 cm from the assembly midplane.

All detector positions as modelled in MCNPX are depicted in Figure 7.

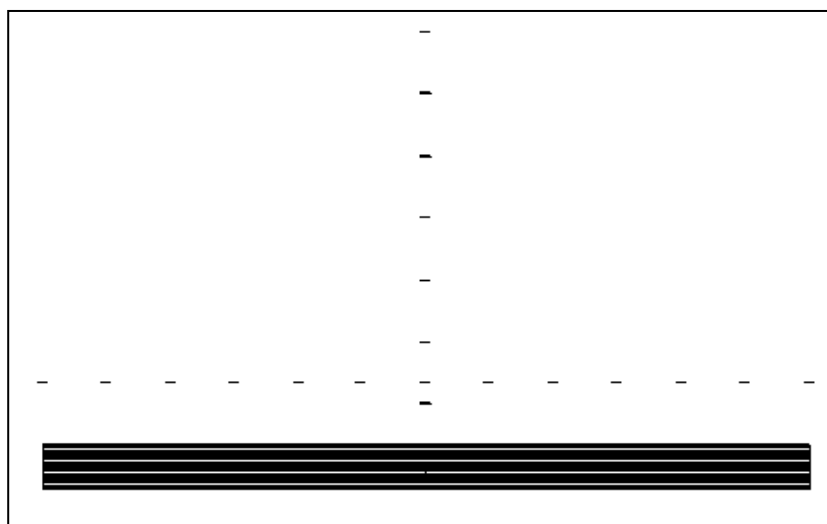


Figure 7. Detector positions as modeled in MCNP.

3.3 Results

Total gamma release rate and contributions from each energy group after a decay of 1.8 years are shown in Table 24.

Group	Photons/s	% of total gammas
1	5.66E+15	32.15
2	1.24E+15	7.01
3	1.74E+15	9.85
4	6.98E+14	3.96
5	7.82E+14	4.44
6	1.06E+15	6.02
7	7.48E+14	4.25
8	3.96E+14	2.25
9	3.86E+15	21.92
10	1.19E+15	6.73
11	1.99E+14	1.13
12	2.29E+13	0.13
13	2.85E+13	0.16
14	5.82E+11	0.00
15	5.28E+10	0.00
16	5.43E+06	0.00
17	6.25E+05	0.00
18	7.19E+04	0.00
Total	1.76E+16	100.00

Table 24. Calculated 1.8-year gamma release rate.

It is important to underline that the gamma release rate is calculated considering the decay between the two intermediate cycles of 58 and 62 days, respectively. In the event that these decay periods were not taken into account, the photon source would be about 5% higher (i.e. $1.85E+16$ photons/s).

Above 0.4 MeV, i.e. at the emission energies relevant in this study (that, as discussed in chapter 2.3.1, are due to the combination of the fuel attenuation and conversion model), the energy distribution is dominated by photons in groups #9 and #10 representing approximately 29% of the total photon emission.

The accuracy of the value calculated by means of this 18 energy group structure is checked through an *ad hoc* structure in which the most important gamma emitters such as Rh106, Ba137m, Cs134, Pr144 are used to create groups narrow and centered around their emission energies.

A non-uniform gamma source is modelled in MCNPX in both directions of the fuel region. As for the axial direction, the gamma source is assumed to be proportional to a PWR typical axial burnup distribution corresponding to an average burnup between 26000 – 30000 MWd/MTU [Wagner, 1999]. This distribution, listed in Table 25, is used to calculate the burnup value and the gamma source probability at each axial height. It is worth noting that if we compare the burnup value of D04-G10 fuel rod “measured” at 167 cm (66 in) from the bottom of the FA [Atkin, 1981] with the value of Table 25 corresponding roughly to the same level (31310 vs 32353 MWd/MTU respectively), the discrepancy is about 3.5%.

Interval number	Upper bound [cm]	Axial burnup distribution	Axial burnup value [MWd/MTU]	Probability
1	20.333	0.551	15665	0.0306
2	40.667	0.886	25189	0.0492
3	61.000	1.007	28629	0.0559
4	81.333	0.974	27691	0.0541
5	101.667	1.146	32581	0.0637
6	122.000	1.138	32353	0.0632
7	142.333	1.140	32410	0.0633
8	162.667	1.135	32268	0.0630
9	183.000	1.138	32353	0.0632
10	203.333	1.166	33149	0.0648
11	223.667	1.173	33348	0.0652
12	244.000	1.173	33348	0.0652
13	264.333	1.169	33235	0.0649
14	284.667	1.157	32894	0.0643
15	305.000	1.022	29055	0.0568
16	325.333	0.882	25075	0.0490
17	345.667	0.701	19929	0.0389
18	366.000	0.444	12623	0.0247
Total		18.002	511797	1
Average burnup [MWd/MTU]			28433	

Table 25. Photon source probability in the axial direction.

As for the radial direction, the gamma source is assumed to be proportional to the radial concentration in the fuel of the most relevant gamma emitters, i.e. Rh106, Cs134, Ba137m, and Pr144. This distribution (rim effect) is calculated in accordance with the following steps:

- ✓ the fuel pellet is split into 20 equal volume regions;
- ✓ the isotopic concentrations are calculated, region by region, at 28430 MWd/MTU by means of APOLLO2. In particular, the concentrations of Rh106, Pr144 and Ba137m (not being contained in the depletion chains of the code) are calculated by the quantity of their parents and the half-lives of the radionuclides (Table 26);

Parent	t _{1/2}	Daughter	t _{1/2}
Ru106	374 day	Rh106	30.1s
Ce144	284 day	Pr144	17.29 min
Cs137	30 year	Ba137m	2.55 min

Table 26. Half-lives of parents and daughters.

- ✓ finally, the concentration of all relevant isotopes in one region (in other terms, the gamma source of that region) is normalized to the value of total concentration.

The total concentration of the four isotopes taken into account and the corresponding gamma source probability are shown, region by region, in Table 27.

Region	Outer radius [cm]	Total concentration [at.]	Probability
1	0.1060	3.66E+18	0.0438
2	0.1500	3.69E+18	0.0441
3	0.1837	3.71E+18	0.0444
4	0.2121	3.74E+18	0.0447
5	0.2371	3.77E+18	0.0451
6	0.2597	3.80E+18	0.0454
7	0.2805	3.83E+18	0.0458
8	0.2999	3.86E+18	0.0462
9	0.3181	3.90E+18	0.0467
10	0.3353	3.94E+18	0.0471
11	0.3517	3.98E+18	0.0476
12	0.3673	4.03E+18	0.0482
13	0.3823	4.08E+18	0.0489
14	0.3967	4.14E+18	0.0496
15	0.4107	4.22E+18	0.0505
16	0.4241	4.32E+18	0.0516
17	0.4372	4.45E+18	0.0533
18	0.4499	4.67E+18	0.0559
19	0.4622	5.12E+18	0.0613
20	0.4742	6.65E+18	0.0796

Table 27. Photon source probability in the radial direction.

The comparison between measurements (M) and calculations (C) is discussed below. The values of gamma dose rate in the axial and radial directions are shown in Table 28 and Table 29 respectively. The corresponding curves are plotted in Figure 8 and Figure 9.

It should be noted that the uncertainties of the measured values are based on statistical counting errors and are at the most 9% [Willingham, 1981]. Uncertainty values equal to a standard deviation (1σ) are available in [Davis, 1980] but only for the radial measurements (see Table 29). As for the calculations, the uncertainty values correspond to one standard deviation.

Distance from the bottom of FA [cm]	Gamma dose rate [Sv/h]			Relative difference [%]	
	Measured	Calculated with ANSI/ANS-6.1.1-1977	Calculated with ANSI/ANS-6.1.1-1991	C(ANSI1977) vs M	C(ANSI1991) vs M
30	74.2	59.3 ±0.6	47.5 ±0.6	-20.1	-36.0
61	121	115.5 ±0.8	92.6 ±0.7	-4.5	-23.4
91	149	147.2 ±0.9	118.1 ±0.8	-1.2	-20.7
122	162	166.6 ±1.0	133.6 ±0.8	2.8	-17.5
152	162	172.2 ±1.0	138.2 ±0.8	6.3	-14.7
183	171	176.8 ±1.1	141.9 ±0.8	3.4	-17.0
213	163	179.6 ±1.1	144.1 ±0.9	10.2	-11.6
244	158	180.4 ±1.1	144.7 ±0.8	14.2	-8.4
274	161	176.5 ±1.0	141.6 ±0.8	9.6	-12.0
305	154	167.0 ±1.0	134.0 ±0.8	8.5	-13.0
335	142	141.7 ±0.9	113.7 ±0.7	-0.2	-19.9
366	110	99.6 ±0.8	79.9 ±0.6	-9.4	-27.3
396	72.9	52.0 ±0.6	41.2 ±0.5	-28.6	-43.4

Table 28. Measured and calculated gamma dose rates along the axial direction.

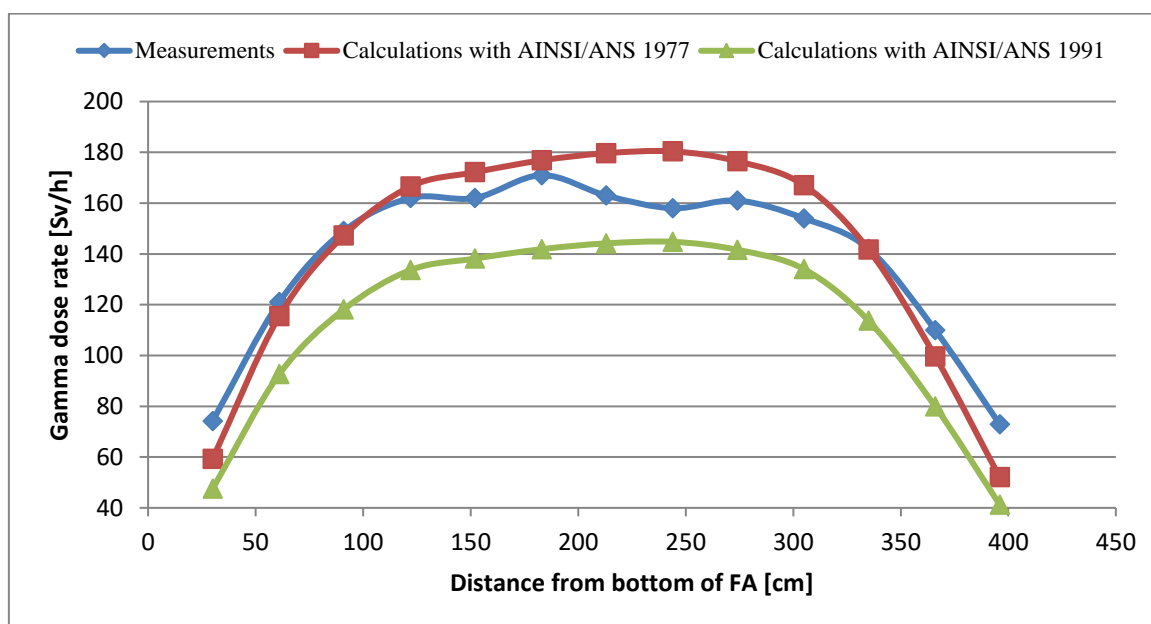


Figure 8. Comparison of the two curves along the axial direction.

Distance from the bottom of FA [cm]	Gamma dose rate [Sv/h]			Relative difference [%]	
	Measured	Calculated with ANSI/ANS-6.1.1-1977	Calculated with ANSI/ANS-6.1.1-1991	C(ANSI1977) vs M	C(ANSI1991) vs M
31	186 ±5.6	256.2 ±1.3	205.5 ±1.0	37.7	10.5
61	98.8 ±3	108.7 ±0.8	87.3 ±0.7	10.1	-11.7
91	68.1 ±3.4	63.6 ±0.6	51.0 ±0.5	-6.6	-25.1
122	49.1 ±2	41.2 ±0.5	33.1 ±0.4	-16.0	-32.6
152	39.2 ±1.6	28.2 ±0.4	22.6 ±0.3	-28.2	-42.4
183	33.4 ±1	21.8 ±0.4	17.5 ±0.3	-34.6	-47.6
213	28.5 ±0.6	16.1 ±0.3	12.9 ±0.2	-43.4	-54.6
244	22.4 ±0.9	12.6 ±0.3	10.1 ±0.2	-43.7	-54.9

Table 29. Measured and calculated gamma dose rates along the radial direction.

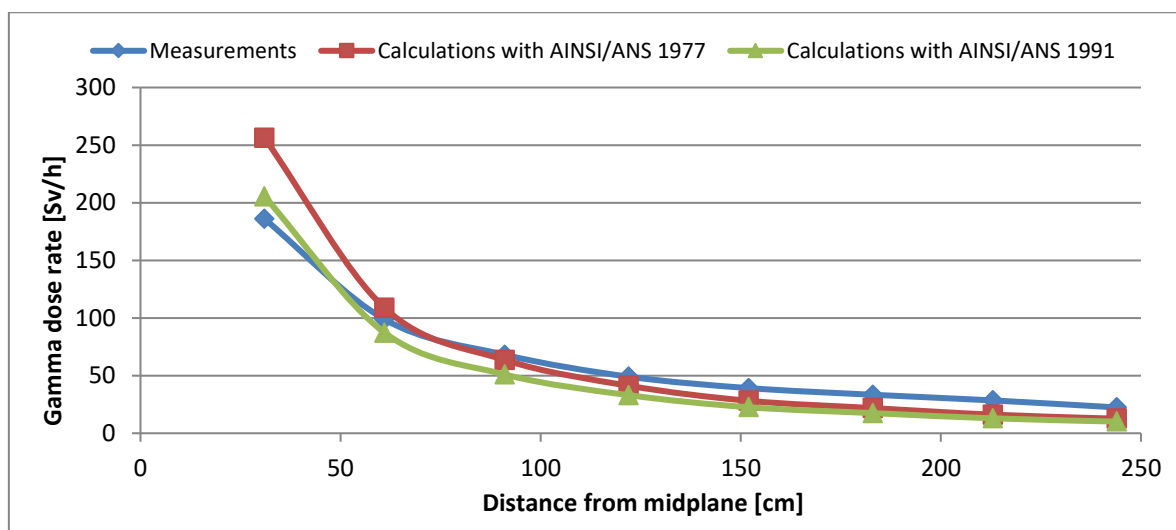



Figure 9. Comparison of the two curves along the radial direction.

In both directions, the values of gamma dose rate for the ANSI/ANS-6.1.1-1977 conversion factor are around 20% higher than those for the ANSI/ANS-6.1.1-1991 conversion factor. Compared to the values measured, the following can be observed:

- ✓ in axial direction, the gamma dose rates for the ANSI/ANS-6.1.1-1977 conversion factor show an overestimation at the middle of the assembly with a maximum relative difference of +14.2% and an underestimation at the axial ends of the assembly with a maximum relative difference of -28.6%;
- ✓ in axial direction, the gamma dose rates for the ANSI/ANS-6.1.1-1991 conversion factor show an general underestimation. In this case, the discrepancy varies from -8.4% to -43.4% going from the middle to the axial ends of the fuel assembly;
- ✓ in radial direction, the results for both conversion factors show an overestimation in the detectors closest to the assembly and an increasing underestimation moving away from the assembly with relative differences reaching -43.7% and -54.9% for ANSI/ANS-6.1.1 conversion factors of 1977 and 1991, respectively.

 Centro Ricerche Bologna	Sigla di identificazione	Rev.	Distrib.	Pag.	di
	SICNUC-P000-026	1	L	30	34

4. Conclusions

ENEA's results to the WPCF/AFCS Expert Group benchmark on dose rate calculations are summarised below.

In the verification part, a good agreement is observed in terms of nuclide inventory, gamma source and gamma dose rate between the five calculation strategies used to compare the performance of the codes. Furthermore, the gamma dose rate value at 1 m from the centre of a spent PWR UOX FA after a cooling time of 30 year is found to be between 2 and 3 times lower than that estimated by [Llyod, 1994].

In the validation part, the gamma dose rate measurements performed on a Westinghouse 15x15-21LOPAR UOX fuel assembly are used to validate the calculation strategies developed in the previous part. The calculations are performed with Origen-S for the depletion and decay phases and with MCNPX for photon transport. The gamma dose rate values for the ANSI/ANS-6.1.1-1977 conversion factor differ by approximately 20% from those for the ANSI/ANS-6.1.1-1991 conversion factor. The relative differences between calculated and measured dose rates vary widely with the position of the detector. In the case of the ANSI/ANS-6.1.1-1977 conversion factor, this discrepancy goes from +14.2% to -28.6% in the axial direction and from +37.7% to -43.7% in the radial direction. In the case of the ANSI/ANS-6.1.1-1991 conversion factor, it ranges from -8.4% to -43.4% in the axial direction and from +10.5% to -54.9% in the radial one. Overall, these results show an acceptable agreement between measurements and calculations.


Appendix I – AINSI/ANS-6.1.1 Flux-to-dose conversion factors

AINSI/ANS-6.1.1-1977		AINSI/ANS-6.1.1-1991	
Photon energy [MeV]	[Sv/h/ph/cm ² s]	Photon energy [MeV]	[Sv/h/ph/cm ² s]
0.01	3.96E-08	0.01	2.21E-10
0.03	5.82E-09	0.013	4.41E-10
0.05	2.90E-09	0.016	6.45E-10
0.07	2.58E-09	0.02	8.58E-10
0.10	2.83E-09	0.025	1.04E-09
0.15	3.79E-09	0.03	1.15E-09
0.20	5.01E-09	0.04	1.29E-09
0.25	6.31E-09	6.00E-02	1.47E-09
0.30	7.59E-09	8.00E-02	1.67E-09
0.35	8.78E-09	1.00E-01	1.91E-09
0.40	9.85E-09	1.50E-01	2.71E-09
0.45	1.08E-08	2.00E-01	3.70E-09
0.50	1.17E-08	2.50E-01	4.68E-09
0.55	1.27E-08	3.00E-01	5.63E-09
0.60	1.36E-08	4.00E-01	7.44E-09
0.65	1.44E-08	6.00E-01	1.08E-08
0.70	1.52E-08	8.00E-01	1.38E-08
0.80	1.68E-08	1.00E+00	1.65E-08
1.00	1.98E-08	1.20E+00	1.90E-08
1.40	2.51E-08	1.50E+00	2.25E-08
1.80	2.99E-08	2.00E+00	2.77E-08
2.20	3.42E-08	2.50E+00	3.24E-08
2.60	3.82E-08	3.00E+00	3.69E-08
2.80	4.01E-08	4.00E+00	4.50E-08
3.25	4.41E-08	5.00E+00	5.27E-08
3.75	4.83E-08	6.00E+00	6.01E-08
4.25	5.23E-08	8.00E+00	7.46E-08
4.75	5.60E-08	1.00E+01	8.92E-08
5.00	5.80E-08	1.20E+01	1.04E-07
5.25	6.01E-08		
5.75	6.37E-08		
6.25	6.74E-08		
6.75	7.11E-08		
7.50	7.66E-08		
9.00	8.77E-08		
11.00	1.03E-07		
13.00	1.18E-07		
15.00	1.33E-07		

Appendix II - Energy group structures

Group	$E_{min} - E_{max}$ [MeV]		
	18 group	19 group	62 group
1	0.00-0.02	0.00-0.05	0.01-0.10
2	0.02-0.03	0.05-0.07	0.10-0.30
3	0.03-0.05	0.07-0.11	0.30-0.40
4	0.05-0.07	0.11-0.16	0.40-0.45
5	0.07-0.10	0.16-0.23	0.45-0.50
6	0.10-0.15	0.23-0.34	0.50-0.55
7	0.15-0.30	0.34-0.51	0.55-0.60
8	0.30-0.45	0.51-0.75	0.60-0.63
9	0.45-0.70	0.75-1.25	0.63-0.65
10	0.70-1.00	1.25-1.75	0.65-0.68
11	1.00-1.50	1.75-2.25	0.68-0.70
12	1.50-2.00	2.25-2.75	0.70-0.73
13	2.00-2.50	2.75-3.50	0.73-0.75
14	2.50-3.00	3.50-4.50	0.75-0.78
15	3.00-4.00	4.50-5.50	0.78-0.80
16	4.00-6.00	5.50-6.50	0.80-0.82
17	6.00-8.00	6.50-7.50	0.82-0.84
18	8.00-11.00	7.50-8.65	0.84-0.86
19	-	8.65-20.00	0.86-0.88
20	-	-	0.88-0.90
21	-	-	0.90-0.92
22	-	-	0.92-0.94
23	-	-	0.94-0.96
24	-	-	0.96-0.98
25	-	-	0.98-1.00
26	-	-	1.00-1.05
27	-	-	1.05-1.10
28	-	-	1.10-1.15
29	-	-	1.15-1.20
30	-	-	1.20-1.25
31	-	-	1.25-1.30
32	-	-	1.30-1.35
33	-	-	1.35-1.40
34	-	-	1.40-1.45
35	-	-	1.45-1.50
36	-	-	1.50-1.55
37	-	-	1.55-1.60
38	-	-	1.60-1.65
39	-	-	1.65-1.70
40	-	-	1.70-1.77
41	-	-	1.77-1.85
42	-	-	1.85-1.92

43	-	-	1.92-2.00
44	-	-	2.00-2.10
45	-	-	2.10-2.20
46	-	-	2.20-2.30
47	-	-	2.30-2.40
48	-	-	2.40-2.50
49	-	-	2.50-2.60
50	-	-	2.60-2.70
51	-	-	2.70-2.80
52	-	-	2.80-3.00
53	-	-	3.00-3.25
54	-	-	3.25-3.50
55	-	-	3.50-3.75
56	-	-	3.75-4.00
57	-	-	4.00-4.50
58	-	-	4.50-5.00
59	-	-	5.00-6.00
60	-	-	6.00-7.00
61	-	-	7.00-8.00
62	-	-	8.00-10.00

 Centro Ricerche Bologna	Sigla di identificazione	Rev.	Distrib.	Pag.	di
	SICNUC-P000-026	1	L	34	34

References

- [Atkin, 1981] S. D. Atkin, *Destructive examination of 3-cycle LWR fuel rods from Turkey Point unit 3 for the climax*, Hanford Engineering Development Laboratory, June 1981.
- [Davis, 1980] R. B. Davis et al., *Remote characterization of spent LWR fuel for geological disposal demonstration*, American Nuclear Society, March 1980.
- [Eschbach et al, 2015] R. Eschbach et al, *Proposal for a Benchmark on Dose Rate Calculations for Irradiated Assemblies by the WPFC/AFCS Expert Group*, 2015.
- [Feng, 2014] B. Feng, R. N. Hill, R. Girieud, R. Eschbach, *Comparison of Gamma Dose Rate Calculations for PWR spent Fuel Assembly*, Physor 2014.
- [Lloyd, 1994] W.R. Lloyd, M.K. Sheaffer, W.G. Sutcliffe, *Dose Rate Estimates from irradiated Light-Water-Reactor Fuel Assembly in Air*, LLNL UCRL-ID-115199, 1994.
- [NAS, 1994] NAS, *Committee on International Security and Arms Control, Management and Disposition of Plutonium*, National Academy Press, 1994.
- [Nichol, 1997] M. Nichol, *SAS2H Analysis of Radiochemical Assay Samples from Turkey Point PWR Reactor*, B0000000-01717-0200-00141 REV 00, CRWMS/M&O, February 1997.
- [US-DoE, 1997] US-DoE, *Nonproliferation and Arms Control Assessment of Weapons-Usable Fissile Material Storage and Excess Plutonium Disposition Alternatives*, DOE/NN-0007, 1997.
- [Wagner, 1999] J. C. Wagner, M. D. DeHart, *Review of Axial Burnup Distribution Considerations for Burnup Credit Calculations*, Oak Ridge National Laboratory, 1999.
- [White, 2012] M.C. White, *Further Notes on MCPLIB03/04 and New MCPLIB63/84 Compton Broadening Data For All Versions of MCNP5*, Los Alamos National Laboratory Report LA-UR-12-00018 (2012).
- [Willingham, 1981] C. E. Willingham, *Radiation dose rates from commercial PWR and BWR Spent fuel Elements*, Battelle, October 1981.

Acknowledgments

The Apollo2 code is developed by CEA and co-owned by CEA, EDF and AREVA NP.